SUPPORTING INFORMATION: An all-DNA system close to the percolation threshold

J. Fernandez-Castanon,[1, a)] M. Zanatta,[2] L. Comez,[3] A. Paciaroni,[4] A. Radulescu,[5] and F. Sciortino[1, 6]
[1)] *Sapienza–Università di Roma, P.le A. Moro 5, 00185 Rome, Italy*
[2)] *Dipartimento di Informatica, Università di Verona, 37134 Verona, Italy*
[3)] *CNR-IOM c/o Dipartimento di Fisica e Geologia, Università di Perugia, 06123 Perugia, Italy*
[4)] *Dipartimento di Fisica e Geologia, Università di Perugia, 06123 Perugia, Italy*
[5)] *Jülich Centre for Neutron Science (JCNS) at Heinz Maier-Leibnitz Zentrum (MLZ), Forschungszentrum Jülich GmbH, Garching, Germany*
[6)] *CNR-ISC, UOS Sapienza–Università di Roma, 00186 Rome, Italy*

I. TECHNICAL DETAILS OF SANS EXPERIMENTS

SANS measurements were carried out at the Jülich Centre for Neutron Science (JCNS-MLZ, Garching, Germany) at FRM II on the KWS-2 small-angle neutron diffractometer.[1]

The accessible scattering vector q-range for the experiments went from 0.006 to 0.5 Å^{-1} by using an incident neutron beam wavelength of 5.0 Å, a collimation distance of 8 m and aperture 50×50 mm^2, and two sample-to-detector distances of 1.56 m and 7.56 m. To preserve a good statistics, the exposure times were adjusted depending on the samples' concentration, ranging from 80 min at 1.56 m and 240 min at 7.56 m for the non-diluted sample to 150 min at 1.56 m and 480 min at 7.56 m for the most diluted one. The T was kept constant at 10°C starting the measurements after 45 min of sample thermalization. The sample cells used were quartz Hellma cells of 1 mm path. The scattered intensity for $q > 0.25$ Å^{-1} was found to be constant and comparable to the measured H_2O buffer signal. The experimental data were analyzed according to standard methods considering empty beam, empty cell corrections and buffer subtraction.

II. DESIGN OF THE AB SYSTEM

Four 51-basis long DNA single strands (DNAss) are mixed in equimolar concentrations to self-assemble in tetravalent A units[2–5] (Seq. A1-A4 in Table S1). These sequences are composed by two segments of 20 nucleotides and one segment of 8 nucleotides, separated by adenine basis. Each one of 20-bases segments is designed to be complementary to only one of those present in a different single strand (indicated with the same color in Table S1). This complementarity ensures that the self-assembling mechanisms will lead to the formation of four double helixes by pairing the compatible sections constituting the four arms of the nanoparticle (see Fig. 1 of the manuscript). The length of each arm is approximatively 70 Å. The 8-bases segment constitutes the sticky-end. The adenine bases, not being able to find a complementary basis, (i) form the flexible core of the particle that permits to release stresses in the arms' arrangement[5] and (ii) permit rotation and bending of the sticky sequence.

A similar layout applies to the formation of the bivalent B particles. In this case, two complementary single strand 20-basis long segments (Seq. B1 and B2 in Table S1) are designed to bind in a linear double helix that, being shorter than the persistence length of DNA (≈ 150 basis), can be modelled as a rigid rod. Note that the connector between the two junctions is composed by four groups of double-helix segments joined with four unpaired A bases, originating a semi-flexible junction between the nodes. In addition, the core of the tetra functional A particles is quite flexible, being characterised by two adjacent unpaired A bases per each strand. Both ends of the B particle terminate with a 8-basis long overhangs, labeled in black in Table S1. The A and B sticky ends are programmed to be complementary, thus precluding the formation of undesirable AA or BB bonds. Hence only AB bonds are possible.

The main parameter controlling complementary base pairing is the temperature.[6] The T at which two complementary ssDNA bind together forming a double helix is directly related with the length of the complementary DNA sequences and can be accurately estimated from the theoretical formulation of SantaLucia,[7] implemented in free on-line oligo-calculators such as NUPACK.[8] In a NaCl salt concentration of 200 mM, the A and B particles form at

[a)] Electronic mail: javi.fernandez.castanon@gmail.com

TABLE S1. DNA sequences designed to form A (Seq. $A1 - A4$) and B (Seq. $B1 - B2$) particles.

Seq. A1.	5′-CTACTATGGCGGGTGATAAAAACGGGAAGAGCATGCCCATCCA**GGACACGC**-3′
Seq. A2.	5′-GGATGGGCATGCTCTTCCCGAACTCAACTGCCTGGTGATACGA**GGACACGC**-3′
Seq. A3.	5′-CGTATCACCAGGCAGTTGAGAACATGCGAGGGTCCAATACCGA**GGACACGC**-3′
Seq. A4.	5′-CGGTATTGGACCCTCGCATGAATTTATCACCCGCCATAGTAGA**GGACACGC**-3′
Seq. B1.	5′-GGTTGTGCTTCGCCGTTGCCGA**GCGTGTCC**-3′
Seq. B2.	5′-CGGCAACGGCGAAGCACAACCA**GCGTGTCC**-3′

$T \approx 75$°C. Pairing of the remaining 8 basis-long sticky-ends is predicted to occurs at $T < 60$°C. Hence the formation of the structural component of A and B particles is accomplished before the binding component triggers the association of the individual A and B units. Below $T = 70$ °C , the formed A and B particles will start to link together forming larger ad larger aggregates, that will progressively grow until all possible AB bonds are formed. According to the SantaLucia[7] predictions, in all the experimental conditions all possible AB bonds are formed below $T = 35$ °C. At $T = 10$ °C the expected lifetime[9] of the AB bonds is approximatively 10^4 s.

A. Sample preparation

DNA was synthesized by Integrated DNA Technologies (IDT) with PAGE purification. Thereafter, the sequences were mixed in deionized and filtered H_2O and NaCl buffer whose final concentration was kept constant at 200 mM. Two solutions, one of A at initial concentrations of 191 μM and one of B particles at 598 μM were prepared. NanoDrop[10] measurements confirmed the lack of contaminants. Up to 18 independent NanoDrop measurements confirmed the accuracy (error lower than 4%) of the expected concentrations both for the A and B particles, and of the desired system composition x=0.14.

We allow time after mixing the A and B components to facilitate system equilibration, detected via dynamic light scattering techniques.[9] Specifically, we cool down the sample from 90°C to 10°C in about 8 hours to minimize the presence of incorrect self-assembled structures. Furthermore, before starting the SANS experiments, the system was further equilibrated at 10°C for 45 minutes.

Finally, a sample at $x = 0.14$ (where $x = N_A/(N_A + N_B)$ and N_A (N_B) indicates the number of A (B) particles) and total particles concentration (both A and B particles) $\approx 398\mu$M was prepared. Subsequently, different samples were obtained diluting the original system by factors 2, 3, 6, 8 and 10 whereas the composition x was kept fixed. The dilution factor (inversely proportional to the concentration) will be indicated with the symbol ϕ in the following. A description of the studied samples is listed in Table S2.

TABLE S2. Dilution factor ϕ, and corresponding concentrations ρ_A and ρ_B for each sample. The last two columns indicate the number of A and B particles per liter.

ϕ	ρ_A (μM)	ρ_B (μM)	$N_A 10^{19}/liter$	$N_B 10^{19}/liter$
As prepared	56.46	341.16	3.4	20.5
2	28.23	170.58	1.7	10.25
3	18.82	113.72	1.13	6.83
6	9.41	56.86	0.56	3.42
8	7.06	42.65	0.43	2.56
10	5.65	34.12	0.34	2.05

Finally, to double check that sedimentation effects during the measurements can be neglected we have measured by DLS the time evolution of the density fluctuations before and after centrifugation and found no differences neither in the signal intensity, nor in the measured timescale. In addition, the absence of radiation damage was discarded by DLS measurements performed before and after the SANS experiments, finding identical results.

III. MELTING PROFILES AT DIFFERENT DILUTION CONDITIONS

The theoretically calculated[8] melting profiles for the investigated dilution factors are presented in Fig. S1 (a) reporting the fraction of unpaired bases of the A and B sticky sequences as a function of the temperature T between 5°C and 90°C for all studied dilutions.

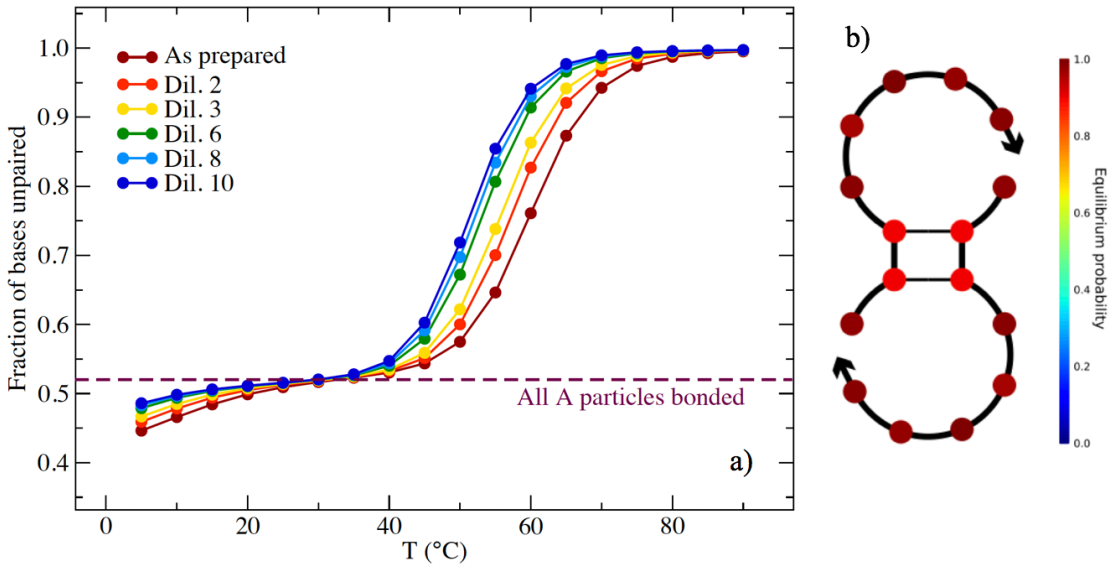

FIG. S1. Evolution of base pairing under different dilution conditions. (a) Melting temperature profiles, revealing the fraction of unpaired bases as a function of the temperature. The dashed line indicates the point at which all the A units are fully bonded to B particles. (b) At temperatures lower than 20°C, some weak BB bonding events occur via the bonding of the two central bases of the B sticky-ends, which does not affect the overall configuration of the network and the A particles remain fully-bonded.

As expected, at $T > 80$°C, all the bases are unpaired. The bonding process starts around 70°C and it reaches completion around $35 - 40$°C depending on the dilution. Below $T = 35$°C, a clear plateau, equal for all the dilution conditions investigated, emerges. In this condition, all the A particles ends are complemented by B sticky ends, indicating a state of fully-bonded A particles. NUPACK indicates that some further pairing starts at $T < 20°$. This additional bondings reflects a weak two-bases BB pairing that takes places between free (not part of clusters) B particles. This two-bases weak bonding is shown in Fig. S1(b).

IV. IMAGES OF THE ABA LINK

To provide a qualitative picture of the flexibility of the link between network nodes we have simulated a bonded ABA system with oxDNA[11] at the experimental temperature and salt concentration. Fig. S2 reports snapshots from the simulation highlighting the flexibility introduced by the four unpaired A bases along the link and the A particle flexible core. The unpaired A bases are coloured in green.

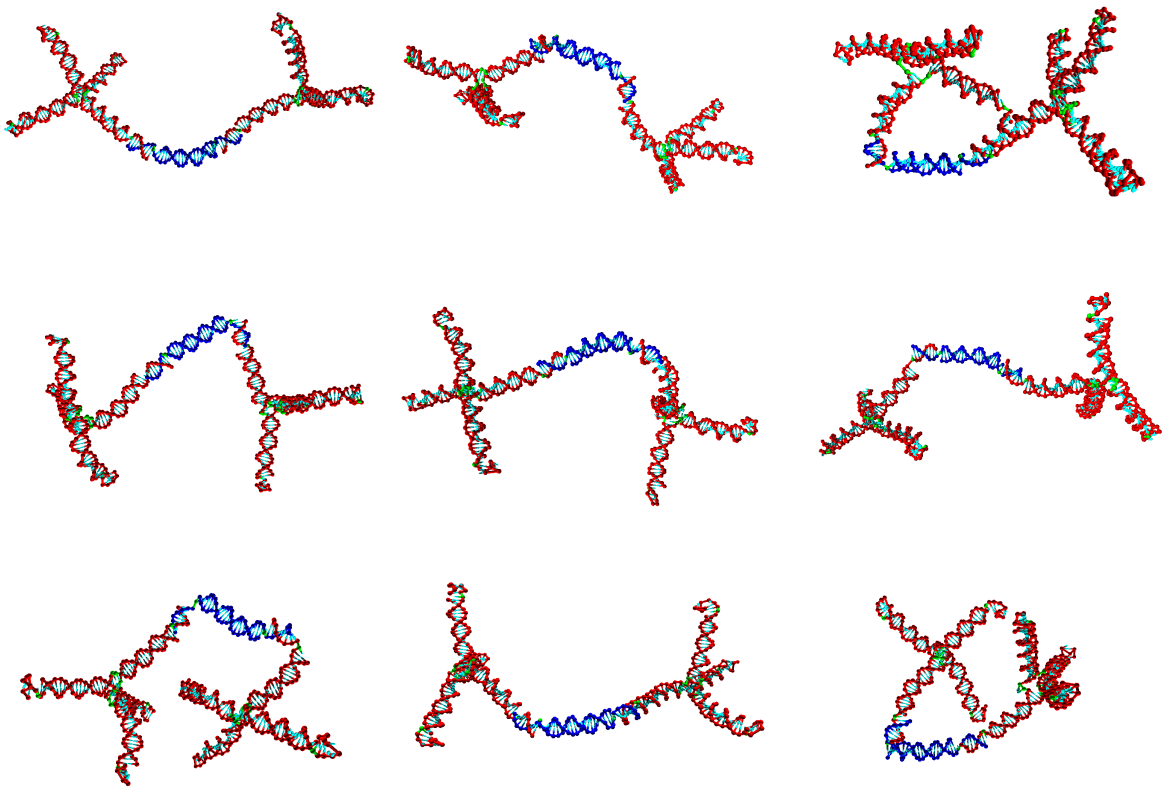

FIG. S2. Snapshots extracted from a simulation of a bonded ABA triplet based on the oxDNA interaction potential model.[11] The A particles are coloured in red, the B particle is coloured in blue. The unpaired adenine bases which provide flexibility to the linking sequence are coloured in green. The adenine unpaired bases located at the core of the A particle are also indicated in green.

REFERENCES

[1] Radulescu, A.; Pipich, V.; Frielinghaus, H.; Appavou, M.-S. KWS-2, the high intensity/wide Q-range small-angle neutron diffractometer for soft-matter and biology at FRM II. *J. Phys. Conf. Ser.* **2012**, *351*, 012026.

[2] Seeman, N. C. At the crossroads of chemistry, biology, and materials: structural DNA nanotechnology. *Chem. Biol.* **2003**, *10*, 1151.

[3] Seeman, N. C. DNA in a material world. *Nature* **2003**, *421*, 427.

[4] Li, Y.; Tseng, Y. D.; Kwon, S. Y.; d'Espaux, L.; Bunch, J. S.; McEuen, P. L.; Luo, D. Controlled assembly of dendrimer-like DNA. *Nat. Mat.* **2004**, *3*, 38.

[5] Biffi, S.; Cerbino, R.; Bomboi, F.; Paraboschi, E. M.; Asselta, R.; Sciortino, F.; Bellini, T. Phase behavior and critical activated dynamics of limited-valence DNA nanostars. *PNAS* **2013**, *110*, 15633.

[6] Chalikian, T. V.; Völker, J.; Plum, G. E.; Breslauer, K. J. A more unified picture for the thermodynamics of nucleic acid duplex melting: a characterization by calorimetric and volumetric techniques. *PNAS* **1999**, *96*, 7853–7858.

[7] SantaLucia, J. A unified view of polymer, dumbbell, and oligonucleotide DNA nearest-neighbor thermodynamics. *PNAS* **1998**, *95*, 1460–1465.

[8] Zadeh, J. N.; Steenberg, C. D.; Bois, J. S.; Wolfe, B. R.; Pierce, M. B.; Khan, A. R.; Dirks, R. M.; Pierce, N. A. NUPACK: analysis and design of nucleic acid systems. *J. Comp. Chem.* **2011**, *32*, 170–173.

[9] Fernandez-Castanon, J.; Bomboi, F.; Sciortino, F. Binding branched and linear DNA structures: From isolated clusters to fully bonded gel. *J. Chem. Phys.* **2018**, *148*, 025103.

[10] Desjardins, P.; Conklin, D. NanoDrop microvolume quantitation of nucleic acids. *Journal of visualized experiments: JoVE* **2010**,

[11] Šulc, P.; Romano, F.; Ouldridge, T. E.; Rovigatti, L.; Doye, J. P. K.; Louis, A. A. Sequence-dependent thermodynamics of a coarse-grained DNA model. *J. Chem. Phys.* **2012**, *137*, 135101.